Applied Energy 241 (2019) 625–639

Contents lists available at ScienceDirect

Applied Energy

journal homepage: www.elsevier.com/locate/apenergy

Integration of energy markets in microgrids: A double-sided auction with device-oriented bidding strategies

Wessam El-Baz*, Peter Tzscheutschler, Ulrich Wagner

Institute of Energy Economy and Application Technology, Technical University of Munich, Arcisstr. 21, 80333 Munich, Germany

HIGHLIGHTS

- A market model for energy trading and energy management of Microgrids is described.
- Device-oriented bidding strategies are presented for each device type in buildings.
- PV probabilistic forecast is integrated to demonstrate market dynamics on different type days.
- The utility and prosumers benefit, in addition to the added value of the ICT infrastructure are quantified.

ARTICLE INFO

Keywords:
Microgrid
Island
Grid-connected
Energy market
Peer-to-peer
Energy management systems
Energy trading
Co-simulation

ABSTRACT

Energy trading markets are one of the most viable solutions to incentivize prosumers in Microgrids. They offer the utility a versatile access for flexible loads coordination without violating the consumer privacy. In the literature, several models and designs were presented to address different aspects of energy trading markets, yet there is a gap between these models and their application in real-life. This paper describes a novel discrete-timely double-sided auction model that facilitates energy trading between prosumers in near real-time and forward markets. Since the practical realization of the model represents a crucial criterion for this model, the market is designed with fast clearing mechanism and simple bidding rules that guarantee the benefits of the prosumers, their privacy, and consider their personal preferences. Additionally, a decentralized home energy management approach is followed at the prosumer level to maximize the system reliability and enable an easy integration of multiple devices from different manufacturers. Hence, a device-oriented bidding strategy is demonstrated that considers the physical characteristics and technical limitations of each device type such as electric vehicles (EV), micro-combined heat and power systems (micro-CHP) or heat pumps. Furthermore, an open-source day-ahead probabilistic forecast for the photovoltaic systems (PV) is integrated with a bidding scheme that maximizes the prosumers commitment in the forward market. In the results, field measurements and testbeds data are used to quantify the benefits of the market model to the utility and the prosumers based on different metrics such as self-sufficiency, self-consumption, peak load and CO_2 emission reduction, and total costs. The results indicate that the market model can increase self-sufficiency and self-consumption of a microgrid while reducing the prosumer costs on average by 23%.

1. Introduction

The power grid in Germany has been undergoing substantial transitions since the legislative support for the energy transition plan (Energiewende) was passed in late 2010 [1]. The legislation proposed strategies to increase the renewable energy resources share in energy production and the energy efficiency [2,3]. According to [4], the renewable energy share should represent 60% and 80% of the gross final energy consumption and electricity consumption, respectively. Furthermore, primary energy consumption should be reduced by 20% by 2020 and 50% by 2050. Fixed financial incentives were introduced to renewable energy resources (RES) to deliver on these goals. Additionally, a priority was given to feeding renewable sources in the electricity grid, in order to provide a risk-free environment for investors and new market entrants [5]. Looking at the impact of these policies, renewable energy represented 31.7% of gross electricity consumption and a capacity of 103.6 GW in 2016, compared to 4.2 GW in 1990 [6]. These investments in RES were not just led by the electric power

* Corresponding author.
E-mail address: wessam.elbaz@tum.de (W. El-Baz).

https://doi.org/10.1016/j.apenergy.2019.02.049
Received 13 November 2018; Received in revised form 17 January 2019; Accepted 7 February 2019
Available online 15 March 2019
0306-2619/

Nomenclature

γ	desired cost saving input
φ	desired comfort user input
ϖ	prosumer's profit
β^{α}	accepted bids set
β^{r}	required bids set
Δt	trading time interval
$\dot{Q}$	rate of change of storage content
$\dot{Q}_{CHP}$	CHP thermal power
$\dot{Q}_{DHW}$	domestic hot water demand
	heat pump thermal power
$\dot{Q}_{losses}$	thermal losses
$\dot{Q}_{SH}$	space heating demand
η_{ch}	charging efficiency
η_{dch}	discharging efficiency
κ	CHP coefficient
$\mathcal{B}$	buyers set
$\mathcal{S}$	sellers set
$\mathcal{T}$	trading horizon time set
Ψ	load shifting potential
ρ	density of water
ζ	given probability of PV generation
A_s	storage area
b	buyer or seller bid
C	costs
C_p	heat capacity of water
COP	coefficient of performance
D	prosumer device
E_D	energy required by a device
E_{Batt}	energy content of a battery
h	height of the storage
i	index of buyers
j	index of sellers
k	count of the same bid communication
N	number of market participants
n	number of bids
p	trading price of a buyer or a seller
p^{*}	bid modifed price
p_e	market clearing price
p_{min}	maximum trading price
p_{min}	minimum trading price
Q	energy capacity of a heat storage
q	trading volume of a buyer or a seller
q^{α}	volume of an accepted bid
q_e	cleared volume
q_f	volume of the fixed load
q_g	generated volume
Q_{max}	maximum energy content of the storage
Q_{min}	minimum energy content of the storage
Q_{Set}	set energy content of the storage
t	time
t_d	time of delivery
t_e	latest end time
t_g	time of the gate closure
t_o	operation time
t_r	time to be ready
t_s	start time
T_a	ambient temperature
t_{fh}	trading time horizon
T_{ref}	reference temperature
t_{rest}	resting time between two consecutive operations
T_{su}	supply temperature
T_s	storage temperature

industry but also by households and small-scale consumers. In 2016, households and farms investments share in RES capacity reached 42.5% [7]. This means that the number of prosumers is gradually increasing and so does their impact on the grid.

Conventional grid control methods are outdated given the constraints of the bidirectional flow and the weather-dependent variability of the integrated renewable energy resources. Control of both the generation and demand side is seen as essential for maintaining the stability of the grid. Consequently, demand-side management (DSM) strategies were proposed and evaluated by several researchers to shed or shift consumer loads to serve various goals such as minimizing costs, CO_2 emission or peak loads [8–12].

Home Energy Management Systems (HEMS) are seen as the key solution that enables a DSM in microgrids and households. A HEMS is considered the main communication and control gateway between the device, prosumer, and the utility. Various research projects discussed the optimization techniques and algorithms needed to be deployed in the HEMS. Examples of these techniques and algorithms are stochastic optimization [13], mixed integer quadratic programming [14], mixed integer linear programming (MILP) [8,15], fuzzy logic [10,16,17], and other machine learning techniques [16,18]. Over the last decade, the optimization techniques employed in HEMS applications did not vary, as much as the use-cases on which the model is based. However, several challenges arise when moving from the simulation and modeling environment to the real-life environment. On the utility-side, these challenges relate to scalability, decision decentralization, and guaranteeing the prosumers' reaction; on the prosumer-side, data privacy and fair division of the economic benefit.

At first, a HEMS reacting to real-time price signals seemed to be the optimal solution for solving the challenges faced both the utility and

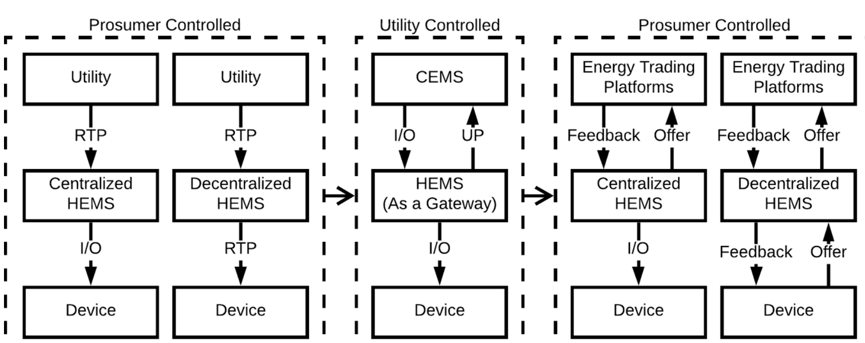

Fig. 1. Development trends of energy management methods in the literature.

prosumers. In such a system, the utility sends a real-time price signal (RTP) that drives the prosumers to shift their load from peak hours to off-peak hours. HEMS load shifting and economic potential were studied from different perspectives and household configurations as in [15,19,20]. These studies and models did address and solve the challenges represented by scalability, decision decentralization, and data privacy, but they did not guarantee the prosumers' reaction to the signal. Assuming that each household has a HEMS that operates autonomously, all the prosumers might switch on their loads or feed energy to the grid at almost the same time. Consequently, the overall results would be the formation of a higher peak at another point in time. Moreover, on the prosumer-side, another challenge was revealed, which is the need for decentralization at the household level as discussed in [9] and the e-MOBILie Project [21,22]. Device manufacturers would not allow direct access to the household device if the device warranty was to be maintained, especially for EVs. Consequently, another architecture was developed based on the RTP that enables decentralized HEMS, where the device handles the decision-making process itself. In this case, the HEMS is used only for communicating the user preferences and initiating the optimization process. Fig. 1 (left) shows the difference between the centralized HEMS and the decentralized HEMS, where I/O is the switching signal forwarded to the device. At the level of an island or grid-connected microgrids, central energy management system (CEMS), which is also referred to as local energy management system (LEMS), was introduced. The CEMS receives all the user preferences (UP) of all prosumers within the microgrid, then tries, based on the algorithms mentioned earlier, to achieve an optimum plan. Such a system can maximize the economic benefits, satisfy the prosumers' constraints, and exploit the maximum flexibility potential. Nevertheless, since the CEMS receives all the user information to start the optimization iterations, it violates the data privacy regulations and exhibits a limited scalability [23,24]. The HEMS, in this case, acts as a gateway. It provides the UP and receives the switching plan of the given devices. Fig. 1 (middle) shows the communication architecture between the HEMS and the CEMS.

Energy trading platforms and market models are the decentralized energy management systems at the microgrid level. They are not only meant for energy trading but also for coordination of the microgrid as discussed in [25]. These platforms solve the privacy challenges faced by the CEMS as they handle the decision-making process without exchanging any detailed information (e.g., EV start time, end time, load). The prosumer has only to decide on the time, volume and price of energy offered. Although the technical realization of these platforms was seen to be somewhat sophisticated and economically infeasible, the development of information and communication technology (ICT) and the pressure imposed by regulations moved research in this direction. In Germany, the new regulations for the digitalization of the energy transition [26] led to investment in the information infrastructure (IIS) and development of the Smart Meter Gateway (SMGW) for maintaining a secure communication channel between the prosumer and the utility. Also, the development and advancement in Blockchain technology revealed the potential for realization of the energy trading platforms.

In the literature, several models are presented tackling the challenges of the energy trading markets within the microgrids. Each research paper focuses on either a specific device or aspect [27–29]. A model that studies the bidding mechanism and integration of every possible prosumer's consuming device (e.g., EV, and HP), generation (e.g., PV and micro-CHPs) or storage was challenging to be realized. In [27], a micro-market was developed for EV in a parking facility. Based on this market, the EVs were allowed to buy and sell to the micro-market depending on their needs and the market situation. [30] studied heat boilers and CHP units integration in the distribution system from the market perspective. The author implemented an optimization model based on deterministic inputs to reach market equilibrium. The model did not consider the capability of the consumers to deliver power, and consequently, the residential users were participating as consumers in the presented market. [31] discussed the pricing schemes of interruptible and uninterruptible electrical appliances, yet the heat side of the prosumer was not considered. Hence, the potential flexibility that can be offered from the heat storage and the operational constraints of thermal systems such as micro-CHPs or heat pumps were not present. [32] presented a two-stage aggregated control framework for peer-to-peer energy trading with a pricing mechanism that ensures the economic benefit of the prosumers. The author focused on PV-Battery Systems in the assessment process, where a reduction of 30% of the bills can be expected and an increase in the annual self-sufficiency by 20%.

The technical constraints and physical characteristics of the devices are not usually modeled [29]. Consequently, the practicality and the possibility of implementation of the presented algorithms are hard to evaluate. Simplified models of the market participants were introduced in the literature to increase the accuracy while minimizing the system complexity. These models lack the dynamics of a real system, which might increase the results' uncertainties.

Several researchers focus on studying energy trading method and framework independent from the nature of the participating devices. In [33], an auction-based market was presented for hour-ahead trading. Within this model, a subscription charge is paid by the user to participate in the platform, which is later used as a price signal to reduce the load on the grid. Kou and Park [34], Zhang et al. [35] applied game theory approaches within their energy trading models. Kou and Park [34] focused on self-organizing microgrids to balance the distribution network, while [35] developed a trading platform (Elecbay) where energy from heterogeneous industrial and residential sources can be traded without an intermediate supplier. In [35], the focus is more on the bidding process of the trading, rather than control of the microgrid. Tushar et al. [36], Millisterfer [37] reviewed the potential of different approaches for energy trading. Tushar et al. [36] focused the game theory approaches in energy trading and applications of cooperative and non-cooperative games, while [37] discussed the current implementation of the energy trading platforms from an international preservative.

In most of the presented models in the literature, the focus was on real-time, near real-time or hour-ahead [33,36–38]. However, forward trading is crucial to exploit the full flexibility potential of the prosumers. Otherwise, the load shifting capability of the prosumer will be confined, which can lessen the economic feasibility of the energy market platforms and their infrastructure. Only a little research discussed forward and real-time trading such as the model of [39], where a bilateral contract network was developed to enable energy trading between prosumers and fuel-based generators. Furthermore, in the published work, centralized HEMS was integrated as in Fig. 1 (left). This architecture, as discussed earlier, is not realizable due to the constraints of the devices manufacturers and their need to have the control algorithms on their own devices.

The forward market models in the literature did not also discuss the prosumer commitment thoroughly in case of a forecast or technical failure. As a convenient solution, [35] proposed that prosumers who failed to generate or supply energy have to be either charged a penalty or trade at lower prices. However, the risk the prosumer is taking and the possible penalties because of the forecast failures were not quantified.

To summarize the status quo of literature and identify research gaps:

- Simple models were used for prosumers devices in households to minimize the required computational power of the market, yet these models can influence the bid volume directly and consequently the market dynamics.
- Most of the research was focused on either integration of the thermal side or the electrical side of the prosumer, but not both.
- Complicated bidding strategies were applied to develop an optimal bid. These strategies can be hardly deployed in a real-life

environment on the devices as it either requires high computational power or long wait time to communicate with all other market players. Hence, its synchronization with the energy market can be challenging.
- The reviewed models considered centralized HEMS structure and enabled the centralized HEMS to bid directly on behalf of the prosumer and all the devices
- In the reviewed research of forward markets, prosumer commitment was not quantified or evaluated during the market operation.
- Possibilities of integration the state-of-the-art forecast such as probabilistic forecasts were not presented.

The main goal of this paper is to present a model that addresses all the aforementioned gaps and provide a comprehensive solution for the integration of energy markets in microgrids. This model features the following:

- A discrete-timely sealed double-sided auction market with market rules suiting the German context, and a fast clearing mechanism that enables prosumers to trade their energy supply and demand in near real-time and forwards.
- Novel simple non-predictive bidding strategies that is constant, symmetric and pure for each device group to ease its implementation in real-life applications.
- Pricing and bidding scheme for the probabilistic PV prediction systems [40,41].
- Integration of decentralized EMS for trading fixed prosumers' loads and updating the smart devices bids according to the user preferences.
- Experimentally validated devices' models (e.g., [42]) are integrated to provide an accurate bid volume and market dynamics.

As per the recent literature review, no model was presented that integrated all the previously mentioned features. Within the analysis of the model, the prosumer commitment under different prediction uncertainties is evaluated. The prosumers and the utility benefits are quantified based on multiple metrics such as self-sufficiency, self-consumption, peak loads, CO_2 emission and costs. Furthermore, evaluation of the added value of the ICT infrastructure for energy market applications in microgrids.

The structure of the paper is as follows: Section 2 provides an overview of the market design and its operations concept. Section 3 describes the function and bidding strategy of every market component. Section 4 presents the co-simulation environment, integrated models, and their input data. Section 5 demonstrates a case study of 10 residential household microgrid and analyzes the potential of the implemented market model. Section 6 presents a conclusive summary and an outlook for future research.

2. Market design and operations

The literature is rich with multiple markets and auctions design that were discussed and evaluated numerically and experimentally as early as in [43–45]. This literature has set the foundation that is inspiring the recent research developing local energy markets for microgrids [24,46–49]. Although the recent auction-based markets presented in the literature have several standard features, their impact and operation dynamics can be defined through three major criteria: market-clearing rules, bidding rules, frequency and nature of the disseminated information to participants. These criteria define the difference between two different markets models, even if both lie under the same market category [50].

The proposed model in this paper is classified as a discrete-timely sealed double-sided auction with uniform pricing. The double-sided auction by definition is an auction where both buyers and sellers can communicate their bids and asks of standardized commodities as per [51]. In this paper, the bid and ask are referred to as buying and selling bid, respectively.

The market is chosen to be discrete-timely to synchronize all traders communication with the market trading platform and provide a fair environment to all traders where communication speed does not play a role. In discrete-timely auction, the market is cleared at predefined time intervals. However, in continuous-timely auction, the market is cleared as soon as a matching bid is available. Thus, faster traders can have an advantage in continuous-timely auction, which can lead to an inherently flawed auction as per [52]. The trader's speed is not only a function of the decision making speed or even the available computational power but also the communication infrastructure. Given the real-life situation in microgrids, it is practically hard to guarantee a synchronized reaction using continuous-timely auction. Hence, discrete-timely trading is favored in this situation to maintain a fair environment for all the market participants.

The market is chosen to be sealed to maintain the anonymity of the bidder. Consequently, the market players can not learn about the other traders' bids to preserve their privacy. A uniform pricing mechanism is applied as it provides a fair competitive price to all the market participants independent of the given bid price. Moreover, it encourages the suppliers to bid their lowest price to increase their possibility of selling.

The double-sided auction market is designed to enable prosumers to trade their energy in the forward, day-ahead, and intraday independently of the wholesale market. In a smart community with an island or a grid-connected microgrid, the number of participants is denoted by N, where $\{N \in Z^{+}: N \geqslant 2\}$. A market participant can be either a prosumer or the utility. A prosumer can demand deficit energy and act as a buyer i, or supply excess energy and act as a seller j. $i \in \mathcal{B}(t)$ and $j \in \mathcal{S}(t)$, where $\mathcal{B}(t)$ and $\mathcal{S}(t)$ are the time-dependent sets of buyers and sellers, respectively. $t \in \mathcal{T} = \{1, 2, ..., t_{fh}\}$ is the discrete time-step at which trading can occur, where t_{fh} is the length of finite trading horizon. Since it is a discrete-timely market, the trading can occur at any defined time interval Δt. A market participant can communicate multiple bids n with market platform equal to $b_{i,n} = (p_{i,n}, q_{i,n}, t_{d_{i,n}})$, where $p_{i,n}$ is the price of bid n of buyer i, $q_{i,n}$ is the bid volume. $t_{d_{i,n}}$ is the delivery time. $q_{i,n}$ must always be greater than or equal to q_{min}, where q_{min} is the constant minimum quantity of energy that can be traded. In this model, the number of participants is always assumed to be constant at any time t. A market participant can submit a buying or selling bid of zero value, if he is not willing to trade in the market. The bid prices $p_{i,n}$ are formed at the device level depending on the technical constraints and dynamic behavior of the device. In Section 3.3, the bidding strategy and bid formulation will be demonstrated for every device D that can communicate with the market. However, a price ceiling and floor is set for all D participating in the market such that $p_{min} \leqslant p_i, p_j \leqslant p_{max}$. For a grid-connected microgrid, p_{max} and p_{min} can represent the conventional utility energy consumption tariff and feed-in tariff, respectively. The p_{max} can be time-dependent, if real-time tariff (RTP) is applied. The intention behind applying a pricing ceiling and floor is to keep the prices higher than feed-in tariffs for the generators and lower than the utility prices for the consumers at all times t so that the voluntary participation of the prosumers in the microgrid market can be ensured. The readiness of a prosumer to bid higher prices to use the community energy may vary depending on the background and the culture of the society where the market is located. Nevertheless, quantifiable economic gain supported by environmental benefits for the whole of society can attract more prosumers to participate in the market.

Given the high details of the model, Fig. 2 presents a simplified overview of the system design including the market side and the prosumer side. It shows the HEMS, market agent and device controllers on the prosumer side, in addition to the consumption and generation forecasts. A user interface is also available to maintain and receive the user's preferences. IIS is crucial to communicate all the necessary data for the market operation securely. However, IIS requirements are not

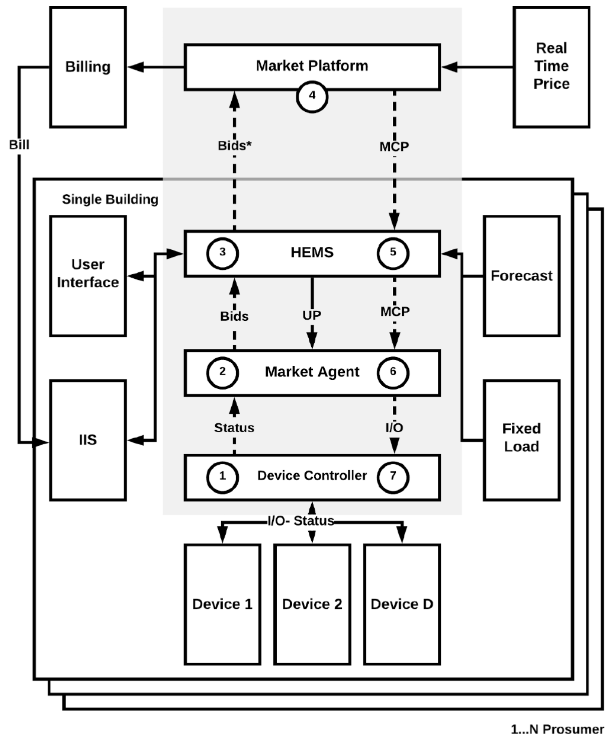

Fig. 2. An overview of the model structure (main communication loop is in gray), circled numbers indicate the communication sequence.

discussed within the framework of this paper. The simplified following communication steps demonstrate the process from forming the bids to the operation of the device once the bid is accepted. These steps are marked in Fig. 2.

Step 1: The device controller sends the status of device D to the market agent.

Step 2: Depending on the device status, user preference and designed bidding strategy, the market agent develops buy or sell bids, b_i or b_j, respectively. Consequently, for each D there is a market agent to maintain a decentralized structure. The bidding strategies are discussed later in Section 3.3.

Step 3: The HEMS receives the bids b_i, b_j from the market agent and modifies it according to the user operation mode (standard, comfort, or cost saving) b_i^*, b_j^*, as in Section 3.2, then it sends them to the market platform.

Step 4: Applying a discrete-timely double-sided auction, the market price and volume at equilibrium are found. The market platform then forwards the market clearing price back to the HEMS. Detailed description is presented in Section 3.1.

Step 5: The HEMS forwards the MCP to the market agents and user through the user interface.

Step 6: The market agent receives the MCP to identify the accepted and rejected bids.

Step 7: The device controller receives the operation signal from the market agent to switch the device at t_d.

3. Market model components

3.1. Market platform

The market platform is the place where all the bids are received to clear the market. In this model, the market platform requires a market coordinator that acts as an auctioneer. The market coordinator can be the utility or the platform owner. The market coordinator roles can be summarized in the following points:

- Clearing the market and announcing the market clearing price.
- Rejecting any bid changes after the gate closure time t_g.
- Balancing the market to guarantee an equilibrium between supply and demand.
- Break the market ties at every trading period.

The first responsibility of the market coordinator to clear the market. It sorts the bids such that $b_{i,n} \geqslant b_{i+1,n}$ for the buyers, $b_{j,n} \leqslant b_{j+1,n}$ for the sellers. The bids are aggregated as step functions $(p_{i,n}, q_{i,n})$ and $(p_{j,n}, q_{j,n})$. The resolution of the step functions can be defined by limiting the maximum bid volume. The intersection of the supply and demand step functions represents the competitive equilibrium and defines the market clearing price value p_e and the cleared volume q_e. The p_e is then communicated to all the prosumers so that they can either operate at t_d or shift their loads to another time. Since the market price has a ceiling and a floor, $p_e \leqslant p_{i,n} \leqslant p_{max}$ for all buyers, and $p_{min} \leqslant p_{j,n} \leqslant p_e$ for the sellers. Hence, the prosumers profit ϖ can be summarized in Eq. (1), where q^α is the volume of the accepted bid.

$$\varpi = \sum_{1}^{n} (p_{max} - p_e) q_{i,n}^{\alpha} + \sum_{1}^{n} (p_e - p_{min}) q_{j,n}^{\alpha} \tag{1}$$

The second responsibility of the market to manage the gate closure time. Since this model enables near real-time and forward trading, a gate closure time has to be defined as a deadline for any changes in bids or withdrawals. Assuming that t_g is set to 30 min, a market participant can make a bid at any t_d in the future and still change the bid up to 30 min before delivery.

The third responsibility of the market coordinator is to balance the market during each trading period in order to clear the market. The prosumers have to guarantee that their energy demand will be covered, even if there is no sufficient supply from the other prosumers in the market. Also, they have to make sure that their non-shiftable generation can be feed-in. Consequently, the market coordinator acts as a seller or a buyer at any period. It sells the deficit energy required by consumers or buys the excess energy produced. Throughout the whole trading time horizon, the market assures that Eq. (2) is maintained.

$$\sum_{i=1}^{\mathcal{B}} \sum_{1}^{n} q_{i,n} = \sum_{j=1}^{\mathcal{S}} \sum_{1}^{n} q_{j,n} \tag{2}$$

The fourth responsibility of the market coordinator is to break the ties to clear the market. Practically, the probability of having market ties is low, yet it is possible. Hence, market breaking ties rules have to be defined. In this model, the market model breaks the ties either randomly, or in the favor of agents bidding the highest volume q_i or q_j. A minimal value of $\varsigma = 1e^{-4}$ is added to the favored agent in order to clear the market.

3.2. Home Energy Management System (HEMS)

As discussed earlier, a decentralized HEMS is needed to maintain the practicality of the model. Conventionally, the HEMS are running optimization algorithms for the devices planning and can be also responsible for the bidding of the prosumer. However, in the project of [21] at the institute for energy economy and application technology (IfE), it was found that these methods are not realizable. Assuming that in a single family household there an EV from manufacturer A and heat pump from manufacturer B. Manufacturer A would not trust manufacture B managing the EV through his own EMS. Also, both do not allow a third party to control their devices. That's why all the products available in the market at the moment are just an interface between the prosumer and the manufacturer cloud.

Building over these experiences, a decentralized structure of HEMS is implemented that allows each market agents to develop its bid independently and communicate it to the market. Decentralized HEMS can not guarantee a global optimum for the prosumer, but a near-optimal solution. The role of the decentralized HEMS can be summarized in the following points:

- Broadcasting the p_e to market agents.
- Bidding for the non-shiftable (fixed loads) based on the load forecast such that $b_{i,n} = (p_{max}, q_f, t_{i,n}^d)$ to guarantee their bids allocation.
- Collecting bids from all market agents (i.e., devices) and forwarding them to the market platform.
- Adjusting the biddings depending on the user preferences.

The users' preferences can vary depending on their interest. Some users are interested in decreasing the costs; others can be more interested in increasing comfort [9,53,54]. The HEMS must adapt the bids to the users' preferences and interests. In this model, the HEMS modifies the bid price $p_{i,n}$ received from the market agent to $p_{i,n}^*$ as in Eq. (3).

$$p_{i,n}^* = \begin{cases} p_{i,n} & \text{if standard} \\ \varphi(p_{max,n} - p_{i,n}) + p_{i,n} & \text{if comfort} \\ max(\gamma(p_{min,n} - p_{max,n}) + p_{i,n}, p_{min,n}) & \text{if cost saving} \end{cases} \tag{3}$$

φ and γ are two variables such that $\{\varphi, \gamma \in \mathbb{R}: 0 \leqslant \varphi, \gamma \leqslant 1\}$. φ and γ could be set by the user to increase or decrease the comfort or cost savings, respectively.

3.3. Market agents

As per [51], double-sided auctions is too complex to output a game-theoretic solution. In this market model, the market agent has no information about the number of bidders, the volume of bids, or the identity of bidders at any trading interval because the market is sealed to maintained the anonymity and data privacy of the prosumers, also to avoid collusion. If a game-theoretic approach would be applied, the market agent has to evaluate all the possible actions for all the market participants in the microgrids to find the solution maximizing its benefit. This strategy would lead to limiting the model scalability given the increasing computational capacity required per market participants. Moreover, as the number of participants increases in this market type, the less influential is market participant (player) actions.

In this model, simple non-predictive bidding strategies are evaluated. Every device group has a symmetric pure constant bidding strategy that do not need a price prediction or complex learning mechanism to develop the bid. The bidding strategy is designed to bid always the truthful price depending on its need. Hence, an agent who is requiring the energy in the next hour would bid more than an agent requiring the energy on the next day. The valuation is always time/need dependent. To optimize the bidding strategy, each agent can submit multiple bids at different time steps within a specific time frame, then use a simple enumeration search optimization technique to find the cheapest accept bid and withdraw/sell the rest additional purchased volume to the market. This concept is applied to each of the typical prosumer flexible devices and tailored to its technical and operational constraints.

The bid development process does not only involve the price but also the volume. Using the non-linear experimentally validated models [42] and the novel probabilistic forecast [40], the exact bidding volume and the corresponding price are evaluated. The accuracy of these models enables to present the realistic dynamics of the market and deliver results comparable to field experiments. In the upcoming sections, the formulation of the bid price and volume is demonstrated for each device type.

3.3.1. Electric vehicle

In this model, the EV is assumed to operate only in the Grid to Vehicle mode (G2V) (i.e., only as a consumer). A user communicating with the HEMS will indicate the desired starting time of the charging t_s and the time by which the vehicle shall be charged and ready t_r. The latest end time is defined as $t_e = t_r - t_o$. The typical charging power is between 3.6 kW (single phase) and 22 kW (three phase) [55].

Assuming a fixed charging power P_{CEV} is required to charge the EV any time between t_s and t_e, the EV market agent sends bids at every possible delivery time t_d between t_s and t_e. The readiness of the market agent to pay more increases linearly as the charging time approaches the t_e as in Eq. (4). After t_e, the market agent always bids a fixed price of p_{max} to ensure the acceptance of the bid either from other prosumers or the utility depending on the market situation.

$$p_{i,n} = \begin{cases} \left(\frac{p_{max} - p_{min}}{t_e - t_s}\right)t_d + p_{min}, & \text{if } t_d \leqslant t_e \\ p_{max}, & \text{if } t_d > t_e \end{cases} \tag{4}$$

The set of accepted bids β_i^α is always larger than the set of required bids $\beta_i^r \subset \beta_i^\alpha$, which is because the market agent creates bids for every period between t_s and t_e and bids the maximum price after t_e.

The market agent selects the most economic bids and withdraws rejected and unneeded bids. As shown in Eq. (5), the bids with the lowest costs are selected such that the number of accepted bids $c(\beta_i^r)$ can satisfy the energy demand E_D of the charging station.

$$min\ C = min_{b_{i,n}^\alpha \in \beta_i^r, \beta_i^r \subset \beta_i^\alpha} \sum b_{i,n}^\alpha = \sum p_{i,n}^\alpha q_{i,n}^\alpha \tag{5a}$$

$$s.\ t.\quad \beta_i^\alpha = \{b_{i,1}^\alpha, b_{i,2}^\alpha, \ldots, b_{i,n}^\alpha\} \tag{5b}$$

$$c(\beta_i^r) < c(\beta_i^\alpha) \tag{5c}$$

$$b_{i,n-1}^\alpha < b_{i,n}^\alpha,\ \forall\ b_{i,n}^\alpha \in \beta_i^\alpha \tag{5d}$$

$$E_D = c(\beta_i^r) q_{i,n}^\alpha \tag{5e}$$

3.3.2. Heat pump

The behavior of heat pumps in the market platform is highly dependent on the heat pump hydraulic configuration, dynamics, modulation, predefined heating curves, and building load. Assuming that the heat pump is installed along with a combi-storage tank that can cover both the space heating (SH) demand and the domestic hot water demand as described in [42], the capacity of the storage Q is defined according to Eq. (6) of [56], where ρ is the density of water, C_p is the heat capacity of water, A_s cross-sectional area of the storage, $T_s(h)$ is the storage at height h and T_{ref} is the reference temperature. In practice, $T_s(h)$ can be measured using a set of sensors across the heat storage as in [42]

$$Q = \rho \times C_p \times A_s \times \int_0^h (T_s(h) - T_{ref})dh\quad \forall\ T_{st}(h) > T_{ref} \tag{6}$$

Depending on the $Q(t)$, predefined set energy content Q_{set} [42], minimum energy content Q_{min} and maximum energy content Q_{max}, the heat pump can develop a bid. Eqs. (7)–(9) can summarize the process of defining the bid volume and price. Then, the market agent selects the optimal bid to minimize the costs in a manner analogous to the EV, Eq. (5).

$$p_{i,n} = \begin{cases} 0, & t < t_{rest} \\ (\frac{p_{max} - p_{min}}{\Psi^-})t_d + p_{min}, & \dot{Q} < 0,\ \text{and } Q_{min} \leqslant Q \leqslant Q_{set} \\ -(\frac{p_{max} - p_{min}}{\Psi^+})t_d + p_{max}, & \dot{Q} > 0,\ \text{and } Q_{min} \leqslant Q \leqslant Q_{set} \\ p_{min}, & Q_{set} < Q \leqslant Q_{max} \end{cases} \tag{7}$$

$$\Psi^- = \frac{Q - Q_{min}}{\dot{Q}_{SH} + \dot{Q}_{DHW} + \dot{Q}_{losses}} \tag{8a}$$

$$\Psi^+ = \frac{Q_{set} - Q}{\dot{Q}_{HP} - \dot{Q}_{SH} - \dot{Q}_{DHW} - \dot{Q}_{losses}} \tag{8b}$$

$$q_{i,n} = COP \times \dot{Q}_{HP} \times \Delta t, \tag{9a}$$

$$where\ \ COP = f(T_{su}, T_a) \approx f(Q, T_a) \tag{9b}$$

$$\dot{Q}_{HP} = f(T_a) \approx f(Q) \tag{9c}$$

t_{rest} is the resting time required between Off and On switch. Ψ^- and Ψ^+ is the negative and positive load shifting potential, respectively. $\dot{Q}$ is the rate of change of storage content. $\dot{Q}_{SH}$ is the space heating load, $\dot{Q}_{DHW}$ is the domestic hot water load. $\dot{Q}_{losses}$ is the thermal losses. is the heat pump thermal power. *COP* is the coefficient of performance of the heat pump. T_{su} is the supply temperature of the heat pump. T_a is the ambient temperature. More details about the technical constraints of the heat pump system, its control, and optimization requirements, in addition to its dynamics and validated model, are available in [42].

3.3.3. Micro-CHP

In this model, the micro-CHP is assumed to have the same hydraulic configuration as the heat pump. Thus, a combi-storage tank is attached to the micro-CHP to cover both the SH and DHW loads. The heat storage Q defines the flexibility of the micro-CHP unless the system configuration enables heat dumping. Consequently, the developed bid price and bid volume can be summarized by Eqs. (10) and (11), where $\varkappa$ is the CHP coefficient, and $\dot{Q}_{CHP}$ is the thermal generation power. Ψ^- and Ψ^+ are calculated as in Eqs. (8).

$$p_{j,n} = \begin{cases} 0, & t_d < t_{rest} \\ -\left(\frac{p_{max} - p_{min}}{\Psi^-}\right)t_d + p_{max}, & \dot{Q} < 0,\ \text{and}\ Q_{min} \leqslant Q \leqslant Q_{set} \\ \left(\frac{p_{max} - p_{min}}{\Psi^+}\right)t_d + p_{min}, & \dot{Q} > 0,\ \text{and}\ Q_{min} \leqslant Q \leqslant Q_{set} \end{cases} \tag{10}$$

$$q_{j,n} = \varkappa \times \dot{Q}_{CHP} \times \Delta t, \tag{11}$$

3.3.4. Photovoltaic

Integration of small-scale PV systems as market suppliers in a day-ahead trading market raises several questions concerning the bid commitment. The commitment of HP, micro-CHP or an EV can be better managed by the prosumer when compared to the PV system. An over forecast in a day-ahead market can lead to an unreal bid and influence the prosumer's future ability to profit from the market, which can directly minimize participation in the market platform.

Typical residential prosumers who have small-scale PV systems with capacities between 1 kWp and 12 kWp are exposed to the highest uncertainties and generation variabilities as discussed in [57]. Fig. 3(b) and (d) show the 1-min resolution measurement of a 3 kWp roof-top PV system. It can be seen that in Fig. 3(b) the PV generation is not exposed to high variabilities compared to Fig. 3(d). Even if the PV forecasting algorithm is able to determine the mean PV profile for days with high variabilities, it would be rather complicated to forecast these variabilities.

El-Baz et al. [40] presented a probabilistic PV generation forecast for HEMS applications and energy market models. The probabilistic PV forecast delivers a range of values depending on $\zeta \in [10\%, 90\%]$. Each value represented a probability of generation of a specific volume as shown in Fig. 3. For the summer day in Fig. 3(a), most of the power forecast lies by $\zeta = 90\%$ and $\zeta = 80\%$. In the transient day shown in Fig. 3(c), the probabilistic forecast was able to forecast the variabilities and indicates the expected power to be generated with lower uncertainties. In [40,57], the model description, validation and demonstration are detailed. The prediction model is also open source and available in [41].

Eq. (12) summaries the bidding strategy of the PV system. The bidding price is formed dependent on ζ. The higher the probability of the generation profile, the lower the price. Thus, the less variable generation will be traded more on the market platform, compared to generation exposed to high variabilities.

$$p_{j,n} = p_{max} + \zeta(p_{min} - p_{max}) \tag{12}$$

Moreover, the prosumer can decide to bid the whole range of ζs or only the guaranteed range (e.g., 80–90%). The forecast delivers only the probabilities, but depending on the prosumers' system and

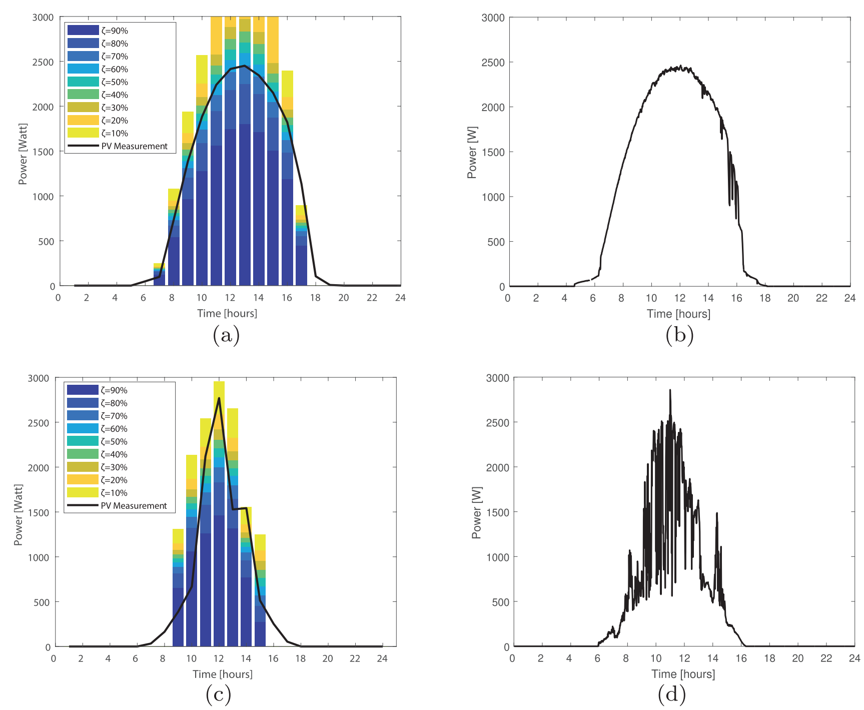

Fig. 3. Selected days of probabilistic forecast output and PV measurements in different seasons, (a) summer (b) summer-1 min resolution (c) transient (d) transient-1 min resolution [40].

configuration, the traded range can be decided. Through this bidding mechanism, the prosumers commitment to the communicated bids can be maximized, and certain bids can be traded. A mean for increasing the traded range is discussed in the next section.

3.3.5. Batteries

In this model, the batteries are considered as a backup system to maximize the prosumers commitment in the market. Assuming that the prosumers have sent a bid, but could not deliver it, the battery discharges to make up for the unfulfilled bid. Eq. (13) relates to the simplified battery charging and discharging behavior depending on the difference between the generated volume q_g and the accepted volume $\sum_1^n q_{j,n}^{\alpha}$, where η_{dch}, η_{ch} are the discharging and charging efficiencies of the battery, respectively.

$$E_{Batt}(t) = \begin{cases} E_{Batt}(t-1) - \frac{1}{\eta_{dch}}(\sum_1^n q_{j,n}^{\alpha} - q_g), & \sum_1^n q_{j,n}^{\alpha} > q_g \\ E_{Batt}(t-1) - \eta_{ch}(\sum_1^n q_{j,n}^{\alpha} - q_g), & \sum_1^n q_{j,n}^{\alpha} < q_g \\ E_{Batt}(t-1), & \text{otherwise} \end{cases} \quad (13)$$

Operation of the battery system under these conditions can make up for the forecast errors and enable the prosumers (i.e., the market agent) to commit to the communicated bid without violating the market rules.

4. Model implementation and co-simulation

The model is co-simulated in two different environments to maximize the model accuracy, and at the same time maintain a proper simulation speed. Fig. 4 shows the models division simulated in the two simulation platforms. The market platform model, billing systems, HEMS, and market agents are integrated into the Matlab model, while SimulationX integrates all the models of the physical devices such as the EV, HP, micro-CHP, or PV, in addition to the building models and the device controllers. The current structure of the model emulates the real-life situation in which a market platform is integrated. All the models running on Matlab can be assumed to be running on cloud as a service, while all the Modelica-based models are real systems.

Although the Matlab market model is scalable and can computed simultaneously on one or multiple computers, the Modelica-based models are limiting the overall model scalability. They are programmed as object-oriented construct of differential algebraic equations (DAEs). Hence, they can present the physical system dynamics accurately, which is necessary for the validation and demonstration of the overall market model in a field test. However, this accuracy comes on the account of the simulation speed and scalability [58]. Modelica and DAEs environments are constrained by the current available solvers such as the CVODE or backward differentiation formula (BDF) solvers [59,60]. Conventionally, these solvers can simulate a single building with multiple energy system. However, the physical models codes were optimized to enable these solvers to simulate up to 15 building model with multiple energy systems.

Replacing the physical models with real hardware eliminates the scalability constraints imposed by Modelica in field tests or real-life implementations. In this case, only the market platform and the billing system are going to be running on a centralized platform. The other model components presented in Fig. 4 are distributed. They are either computed or measured directly at the prosumers.

In this paper, the Modelica-based models are developed and calibrated based on either testbeds or field measurement data. The heat pump model design, and validation, in addition to a demonstration of the testbed, is given in [42]. The micro-CHP model is developed based on the study of [61]. The PV measurements and PV system characteristics are detailed in [62]. The EV models and the buildings used are based on the Green City Package of [63]. A calibration for the building models depending on the IEE Project TABULA [64] was performed to maximize the overall model accuracy. In [42], an example is demonstrated of the nonlinear building, heat storage and heat pump models. The dynamics of these models were compared to the testbed to demonstrate the overall system accuracy. Several metrics were used to evaluate the models dynamically and energetically. For example, the energetic difference between the developed heat pump model and the measured value revealed an error of 3%.

The integrated building model facilitates the evaluation of user comfort. Throughout the simulation process, the temperature profile of each zone of the building model is monitored to make sure that the room temperature never falls below the set temperature tolerance, which is ± 1 K.

The fixed electricity profiles are based on the representative load profiles of [65]. The data includes measured high-resolution profiles of 74 residential houses managed by the same grid operator. The houses are located in the vicinity of each other. Consequently, it can be assumed the given houses lie in the same microgrid.

The hot water profiles are developed based on the standard VDI 4655 for each type day, while hot water circulation load used is based on field measurements of single-family houses in South Bavaria, Germany [66].

5. Case study: microgrid of residential buildings

5.1. Benchmark

A microgrid of 10 single family households is used, where each household has an EV, PV system, and a heat pump. The charging station has a maximum 3.6 kW. The PV system has a 6 kWp. A brine-water heat pump with a thermal power of 10.1 kW and a COP of 5.02 is installed. 10 electrical load profiles are selected from [65] to represent the fixed loads. All the households are assumed to have the same area and thermal load profile. The building models of the prosumers are parameterized based on 1984 building standards. The building parameters can be found in [64] and the building's location is assumed to be Munich, Germany.

Identical user preferences are used in all the households with all the market participants operating using the standard mode as per Eq. (3). The load shifting window of the EV is the same every day, where the difference between t_s and t_r is 24-h.

In this section, a comparison is made between the reference case, where no market platform or HEMS is implemented (conventional operation), and the case with a market platform and the HEMS. Same preferences and characteristics of the household are used to illustrate the market behavior, even in a situation of a simultaneous supply and demand. The comparison is based on a complete analysis of the year 2017.

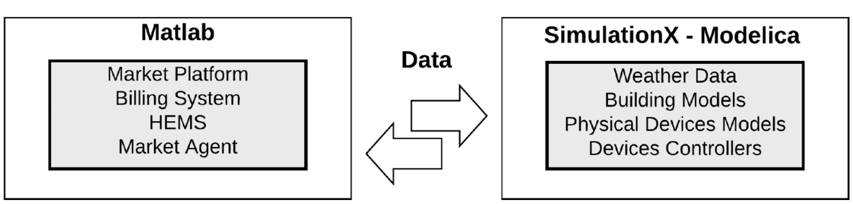

Fig. 4. Model division on the co-simulation platform between Matlab and Modelica.

5.2. Market dynamics

To illustrate the market dynamics and the influence of the prosumer solely on the market price, it is assumed that the utility always participates in the market with a fixed tariff of 0.26 €/kWh and a feed-in-tariff of 0.12 €/kWh as per EEG 2017 [67]. Consequently, p_{max} and p_{min} are equal to 0.26 and 0.12, respectively.

In the case study, the PV system is the sole energy generation system in each prosumers' house. Hence, the MCP is dependent on the PV system as a seller. The MCP falls or rises, depending on whether there is an underproduction, or overproduction from the PV system as shown in Fig. 5. Hence, the mean values of all the summer days are relatively lower than the transient and the winter days. The standard deviation shown in Fig. 5 is in this case dependent on the probabilistic forecast of the given location.

The presented MCP behavior is not standard behavior. It is dependent on the given situation where the utility is providing a fixed tariff, and the prosumers can only sell the PV energy. The analysis of Fig. 5 shows that the market is reacting to the generation conditions and can indicate the demand and supply situation of the microgrid while maintaining the prosumers' privacy. An RTP signal or a whole market price can be used as an input for this model. Also, the utility could be represented by multiple market participants bidding at different prices.

5.3. Utility benefit

The results in Fig. 6 represent the behavior of the microgrid over different type days: summer, transient and winter day. It compares the behavior of the microgrid with and without the market model. The case in which the market platform is not integrated is denoted by the reference.

In the typical summer day shown in Fig. 6(a) and (b), it can be seen that the loads that conventionally operates before the sunrise or the sunset are shifted due to the low market prices to operate during the PV generation hours. An insight about the types of load being shifted can be obtained from Fig. 7(a) and (b). Hence, a reduction in peak loads can be observed. The peak load of the microgrid export is from −58 kW to −39 kW, while the import peak load is reduced from 44.5 kW to 35 kW.

The transient day in Fig. 6(c) and (d) exhibits the same behavior seen in the typical summer day, where the market agents shift the loads to the lowest possible market prices. On this day, the influence of the probabilistic forecast on energy trading is more noticeable since the PV generation is exposed to higher generation variabilities. The probabilistic forecast and its market agent were able to offer the energy with high variability at a price closer to the p_{max} so that other market agents could avoid operation in this period. Hence, it minimizes the exposure of the prosumer to fines for non-delivery. Fig. 7(c) and (d) show a comparison between the behavior of each load in the reference and market model, respectively. It can be seen that most of the heat pumps and EVs operate during the availability of PV generation. However, some EVs shifted their loads to a later time starting at 18:30. In this case, the market agent could not find a cheaper bid less than p_{max} at the PV generation time. Thus, it kept shifting the loads until t_e, waiting for cheaper bids to be offered in the market.

In winter, almost 100% PV generation power is used as shown in Fig. 6(f), compared to Fig. 6(e). The export peak load drops from −46 kW to −11 kW. The import power drops from 60 kW to 43 kW. Due to the high energy consumption of the heat pump in winter, the PV generation does not suffice. Thus, some loads, which are mostly heat pumps, were shifted to a later time of the day, as shown in Fig. 7(f). For all the loads operating after 17:30, the start times are not similar, although they receive the same price and are locally controlled by the market agent. Thus, it can be concluded that the trading process occurred during the PV generation hours on that day desynchronized the loads' operation later at the end of the day and minimized the peaks, even though there are no incentives or motivation for load shifting.

In all the reference model cases in Fig. 7, the heat pumps operate at the same time as the same building model and DHW standard profile are used. In reality, minor differences can be found due to the consumer behavior as discussed in [68]. The EV daily start charging time is based on a normal distribution between 15:00 and 05:00 of the next day.

A one year analysis shows that the market increases the self-sufficiency of the microgrid by 130% and the self-consumption by 120%. Also, it decreases the CO_2 emissions on average by 21% and the import peak load by 25%. The absolute values are discussed for all prosumers in Section 5.4. The presented results not only demonstrate the capability of the market platform to trade, shift the loads but also the accuracy of the probabilistic PV forecast in delivering the profiles that maximize the efficiency of the whole model.

5.4. Prosumer benefit

In this section, a detailed insight into the prosumer benefit is presented. Similarly to Fig. 6, the supply and demand of a single prosumer on the same typical days are presented in Fig. 8. The same conclusions can be drawn for this typical prosumer, in comparison with the reference model. Additionally, the amount of energy traded is shown. The highest energy exchange period was in transient and winter days. In summer, most of the prosumers in the microgrid are using their own generated energies and only a few kWhs can be traded as shown in Fig. 8(b). Furthermore, in transient and winter days, as in Fig. 8(d) and (f), the energy bought and sold are relatively higher due to the increase in the demand of the heat pumps and the decrease in PV generation. Hence, it can be deduced that the lower the capacities available on the prosumer side, the more the prosumers will be depending on each other to trade their energies and shift their loads. Excess capacities will limit the possible amount of energy that can be traded.

The trading dynamics and the behavior of the market agent can be further analyzed based on Fig. 8(d). On that day, the market agent is not only shifting the load depending on the prosumer's own available energy but also depending on the situation in the microgrid. It can be seen that at around 05:30, the market agent bought energy to operate earlier, and sold the generated energy later to the microgrid. On the other hand, it can be shown in Fig. 8(f) that the market agent shifted the load that could be operated starting from 06:00 and sold the energy to the microgrid, to start later at 08:00. In the case of the reference model, the prosumers do not contribute to minimizing the peak load of the microgrid and did not have the opportunity to trade and exchange energy to maximize their economic welfare.

To quantify the benefits for the prosumer, the self-sufficiency, the self-consumption, the peak load, the CO_2 emission, and costs are evaluated for each prosumer in the microgrid over a whole year. Two

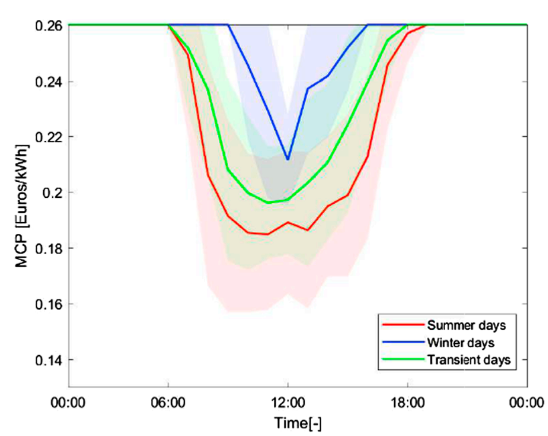

Fig. 5. Market Clearing Price variation in summer days, transient days, and winter days.

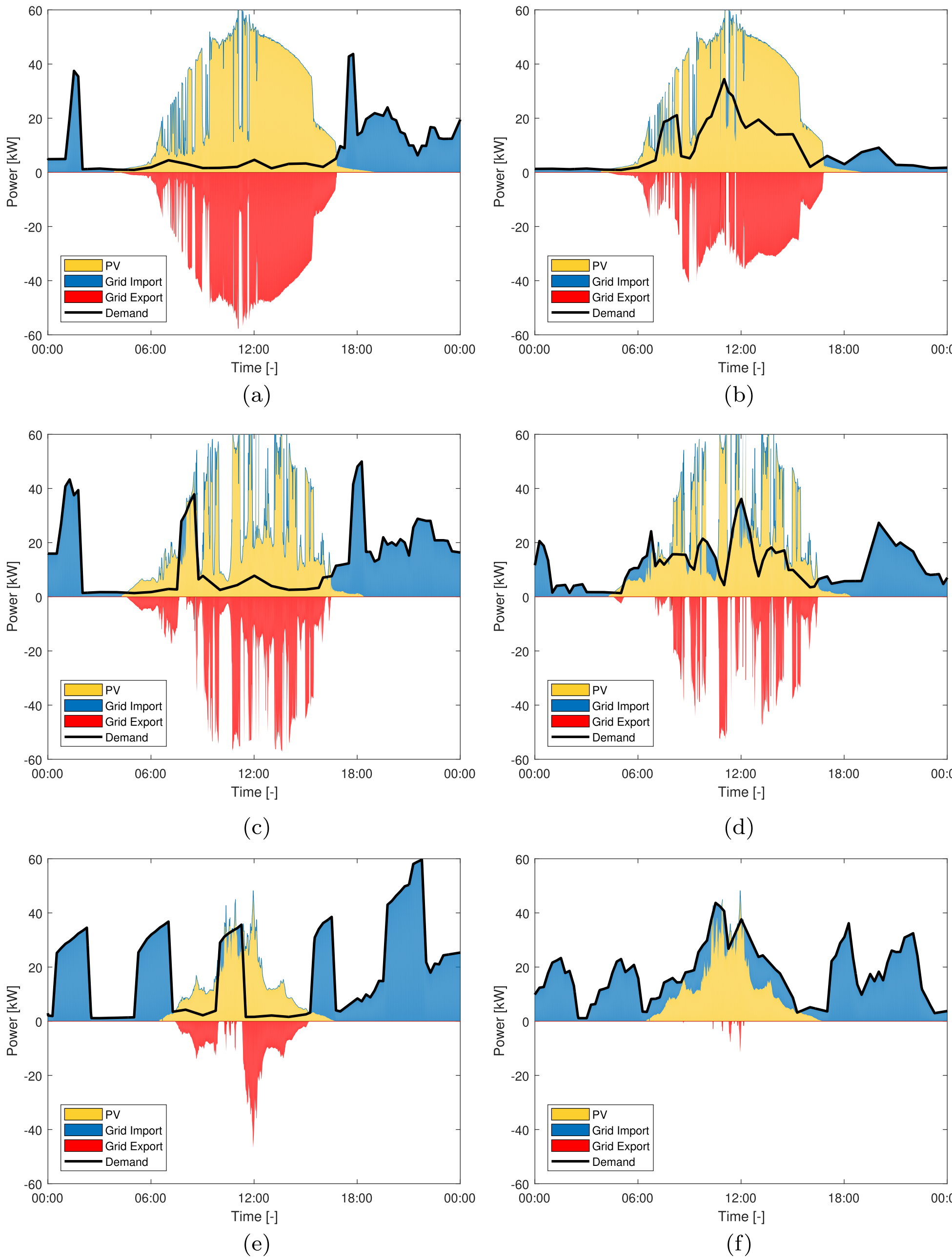

Fig. 6. Type day profile of the whole microgrid, (a) summer day - reference, (b) summer day - market, (c) transient day - reference, (d) transient day - market, (e) winter day - reference, (f) winter day - market.

different costs are assessed: the costs based on the conventional billing systems (CB), and the costs based on the market billing system (MB). In the CB system, the current conventional metering systems (no smart meters) are used such that a fixed price is paid by the prosumer for the energy consumed and a fixed feed-in tariff is received for all the generated energy. In the MB system, the energy generation and consumption prices are decided based on the market price given by Eq. (1). In both cases, the market operations are precisely the same, and the only fundamental difference is the billing. In the case of the CB, it is assumed that a non-certified communication to the market is implemented. The reason for comparing CB and MB is to evaluate the potential added value of the ICT infrastructure (i.e., IIS), as discussed earlier. Also, to assess the potential of applying the market platform immediately (e.g., using micro-computers) without the need of waiting for a smart meter certified billing in Germany.

Fig. 9 shows the distribution of the 10 prosumers under the given metrics for both the market and the reference model. For all the prosumers, the self-sufficiency and self-consumption are higher compared to the reference model. The mean (green) and the median (orange) of the self-sufficiency both increased by 102%. The median of the self-consumption increased by 80% and the mean is slightly higher. Additionally, the median of the peak load decreased by 15%, while the mean decreased by 16%. By evaluating the CO_2 emissions within the boundaries of prosumers' household, the emissions are reduced by 26%.

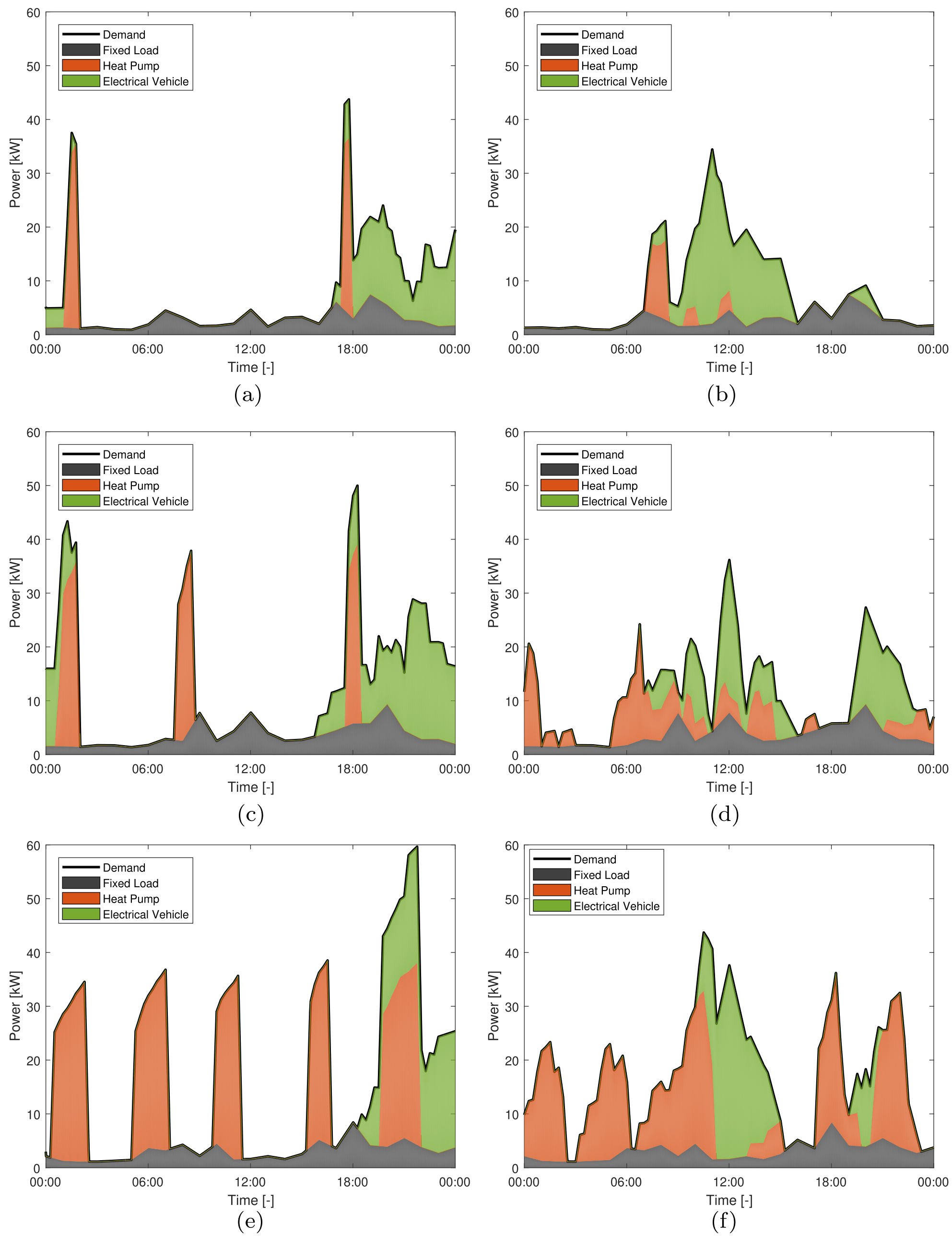

Fig. 7. Detailed demand profile of the microgrid, (a) summer day - reference, (b) summer day - market, (c) transient day - reference, (d) transient day - market, (e) winter day - reference, (f) winter day - market.

Comparing the values of self-sufficiency and self-consumption to the values produced by the centralized energy management algorithm used in [57]. It is found that self-sufficiency and self- consumption are lower using the market platform and decentralized HEMS by 5% and 7%, respectively. Hence, the solution provided is not a global optimal, but a near-optimal solution.

Under both the CB and the MB billing systems, the market demonstrates its ability to minimize prosumer costs. The mean and median costs of the market model are 15% lower than the reference model using the CB, which are equal to 360 euro/a. These costs are based on the current metering infrastructure. Using ICT, the market bid and MCP can be binding. As shown in Fig. 9, the costs of the market model are 23% lower than that of the reference model, and the overall absolute savings are equal to 530 euro/a. Thus, the expected saving from IIS could amount to an additional 170 euro/a in this configuration. These costs were calculated ignoring the transaction and service fees of the grid and market platform operator. Other fees might be considered depending on the regional regulations and the operating costs of the market platform. These costs will not influence the operation plan of the prosumers; in other words, the utility benefits will still be the same, but this would influence the economic benefit of the prosumer. Hence, the market platform operator and the utility must make sure that the economic benefit is maintained within specific boundaries. Otherwise, the prosumers will not be interested in trading

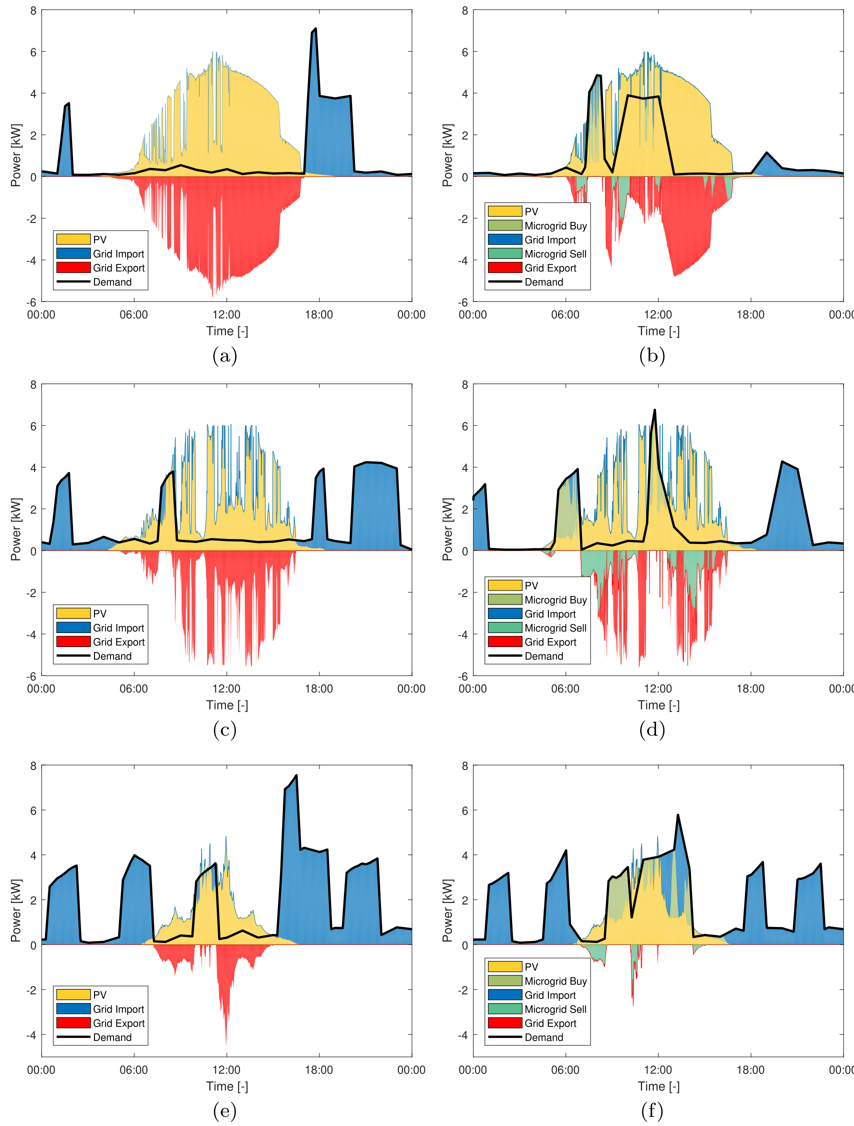

Fig. 8. Type day profile of a typical household in the microgrid, (a) summer day - reference, (b) summer day - market, (c) transient day - reference, (d) transient day - market, (e) winter day - reference, (f) winter day - market.

their energy in the market platform.

Comparing the results of each prosumer to that of the utility, it can be seen that the self-sufficiency, self-consumption or CO_2 emission reduction of average prosumer is lower than that of the whole microgrid. Such a difference is due to the aggregation effect of the load profiles of all the prosumers. However, it is important to demonstrate the benefits share for each prosumer from the participation in the market platform.

The performed analysis assumed that no penalties are paid if the prosumer does not commit to the bid. However, if the prosumer submits a selling bid of a PV system with a $\zeta = 10$, it is probable that the PV system would not be able to deliver the expected bid volume. As discussed in Section 3.3.5, in this situation, the battery system is responsible for fulfilling the bids. Based on a full year analysis, Fig. 10 demonstrates the required battery capacity per kWp PV that the prosumer needs to install to avoid any penalties. For $90 \leqslant \zeta \leqslant 58$, no batteries need to be installed, and 100% of the bids communicated by the PV system can be satisfied. However, the lower the ζ, the higher is the required battery capacity. The optimal battery capacity can only be determined based on the expected platform penalty and the readiness of the prosumer to be exposed to such risks. As discussed, the PV predictions provide an indicator of the certainty of the prediction but do not decide on the amount of energy that can be traded. If the prosumer needs to avoid any penalties, it would be advised to trade up to $\zeta = 60$. With lower ζ, the profit of the prosumer can be increased as indicated by Eq. (12), but penalties might be imposed.

6. Conclusions

In this paper, a market model for energy trading platform is presented in which the prosumers are capable of trading their energy supply and demand. The prosumers communicate with the market via a decentralized HEMS, where each device develops its own bid depending on its physical characteristics and technical constraints. Hence, a bidding strategy is presented for each device type. The models of the integrated devices are based on either field test or testbeds to ensure the accuracy of the integrated model. Moreover, the devices are integrated as non-linear models in the market through a co-simulation platform to demonstrate the system dynamics and maximize their accuracy.

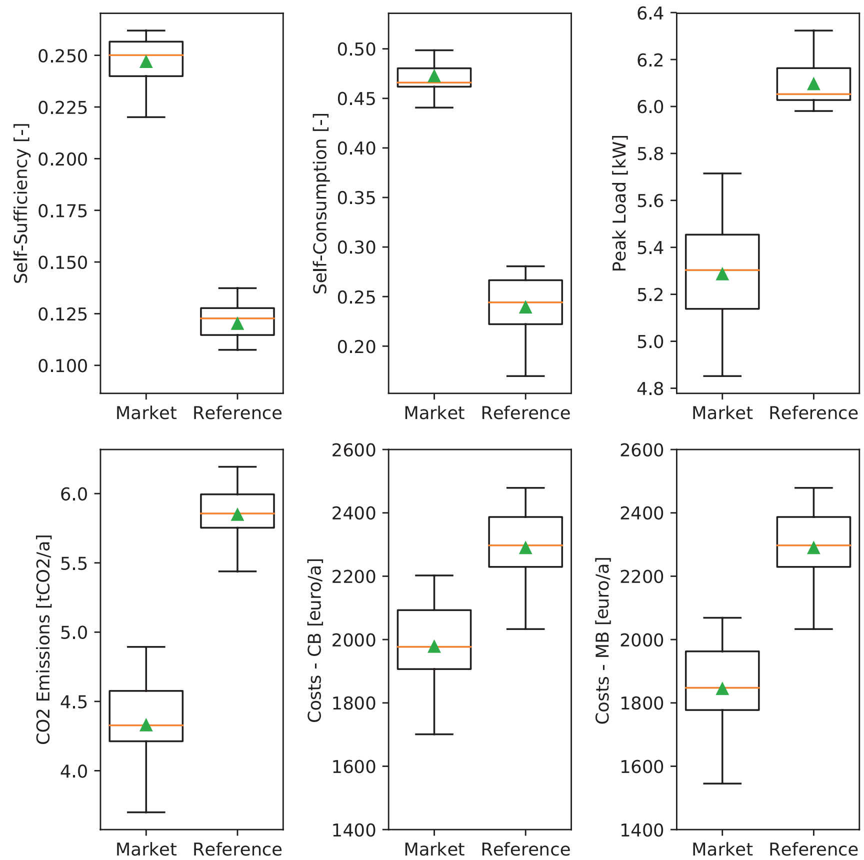

Fig. 9. A comparison between the market and the reference model depending on different metrics.

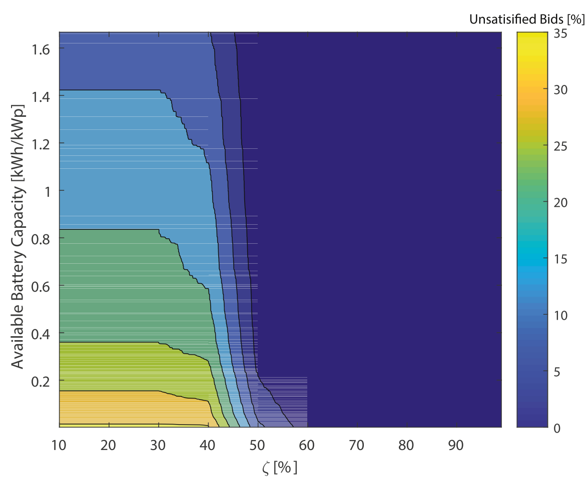

Fig. 10. Percentage of unsatisfied bids against the ζ of the PV prediction and the available battery capacity.

Additionally, a probabilistic PV prediction system is integrated into the market model to show the mechanism of PV energy trading, given its generation uncertainty.

Furthermore, the model allows the prosumers not only to trade in a real-time market but also in a forward market to facilitate energy planning. Hence, the market will benefit both the prosumer and the utility. These benefits can be summarized as follows:

- At the level of the microgrid, the market model doubles the self-sufficiency and self-consumption. CO_2 emissions are reduced by 21%, and the import peak load decreased by 25%. Therefore, it can be concluded that the market not only facilitates energy trading but acts as a microgrid decentralized energy management system as well.
- At the level of the prosumer, it is ensured that benefits are distributed to the market participants. Using the same metrics implemented at the level of the microgrid, the model revealed that the benefit of each prosumer using the market model exceeds that of the reference model.
- Additional metrics are used to evaluate the economic benefit of the prosumers. The costs are calculated based on conventional billing metering infrastructure, then also using the soon-to-be-implemented IIS. In both cases, the prosumers benefits are higher with the market model. Thus, the implementation of the market model can be independent of the current ICT infrastructure. Using conventional infrastructure, the prosumer can save an average of 15% of the costs, while using IIS the prosumer can save 23%.

To maintain the prosumers commitment to the communicated bid, given the uncertainties of renewable generation prediction in the forward market, a battery system is required. The capacity of the battery system and the percentage of unsatisfied bids are calculated depending on the output of the probabilistic forecast model. The results show that the prosumer can participate without having a battery system without being penalized provided that the most probable generation profile is traded.

For future works, a more profound insight will be presented that discuss the factors influencing the market operations. Scenarios evaluating different microgrid and household configuration, pricing mechanisms, and prosumers preferences will be analyzed.

Acknowledgment

This contribution is supported by the Federal Ministry for Economic Affairs and Energy, Bundesministerium für Wirtschaft und Energie, as a part of the SINTEG project C/sells. Responsibility for the content of this publication lies with the authors. The authors are grateful to Johannes Hofbauer from the Institute of Decision Sciences and Systems at the Technical University of Munich for his comments and advice.

References

[1] Renewable Energies Agency. Press fact sheet: the german energy transition, Berlin energy transition dialogue (March); 2016. p. 1–16.
[2] Bundesministrium für Wirtschaft und Energie. BMWi - Erneuerbare Energien; 2017.
[3] Federal Ministry for Economic Affairs and Energy (BMWi). The energy of the future – Foruth energy transition monitoring report summary 2014; 63(4): 60–2.
[4] Federal Ministry of Education and Research. German energy transition – BMBF.
[5] A. Federal Ministry of Food, C. Protection. The Renewable Energy Sources Act.
[6] Federal Ministry for Economic Affairs and Energy (BMWi). Renewable energy sources in figures. National and International Development; 2017. p. 80.
[7] Energy Transition. Share of German citizen renewable energy shrinking.
[8] Barbato A, Carpentieri G. Model and algorithms for the real time management of residential electricity demand. 2012 IEEE international energy conference and exhibition (ENERGYCON) 2012. p. 701–6. https://doi.org/10.1109/EnergyCon.2012.6348242.
[9] El-Baz W, Tzscheutschler P. Co-simulation of a smart home model based on a micro electricity market. Fifth German-Austrian IBPSA conference.
[10] Wu Z, Tazvinga H, Xia X. Demand side management of photovoltaic-battery hybrid system. Appl Energy 2015;148:294–304. https://doi.org/10.1016/j.apenergy.2015.03.109.
[11] Jiang B, Muzhikyan A, Farid AM, Youcef-Toumi K. Demand side management in power grid enterprise control: a comparison of industrial & social welfare approaches. Appl Energy 2017;187:833–46. https://doi.org/10.1016/j.apenergy.2016.10.096.
[12] Aghajani GR, Shayanfar HA, Shayeghi H. Demand side management in a smart micro-grid in the presence of renewable generation and demand response. Energy 2017;126:622–37. https://doi.org/10.1016/j.energy.2017.03.051.
[13] Shen Y, Wen X, Wang L, Guan W. 2018 IEEE international conference on energy internet a visualization compression algorithm considering interactive structure for energy trading of microgrid system. 2018 IEEE international conference on energy internet (ICEI); 2018;(3):49–54. doi:https://doi.org/10.1109/ICEI.2018.00017.
[14] Killian M, Zauner M, Kozek M. Comprehensive smart home energy management system using mixed-integer quadratic-programming. Appl Energy 2018;222(March):662–72. https://doi.org/10.1016/j.apenergy.2018.03.179.
[15] Wang M, Tian L. Regulating effect of the energy market-theoretical and empirical analysis based on a novel energy prices-energy supply-economic growth dynamic system. Appl Energy 2015;155:526–46. https://doi.org/10.1016/j.apenergy.2015.06.001.
[16] Han Y, Zeng Q, Geng Z, Zhu Q. Energy management and optimization modeling based on a novel fuzzy extreme learning machine: case study of complex petrochemical industries. Energy Convers Manage 2018;165(March):163–71. https://doi.org/10.1016/j.enconman.2018.03.049.
[17] Ben Ali I, Turki M, Belhadj J, Roboam X. Optimized fuzzy rule-based energy management for a battery-less PV/wind-BWRO desalination system. Energy 2018;159:216–28. https://doi.org/10.1016/j.energy.2018.06.110.
[18] Guo Y, Wang J, Chen H, Li G, Liu J, Xu C, et al. Machine learning-based thermal response time ahead energy demand prediction for building heating systems. Appl Energy 2018;221(November 2017):16–27. https://doi.org/10.1016/j.apenergy.2018.03.125.
[19] Gottwalt S, Ketter W, Block C, Collins J, Weinhardt C. Demand side management: a simulation of household behavior under variable prices. Energy Policy 2011;39(12):8163–74. https://doi.org/10.1016/j.enpol.2011.10.016.
[20] Chen Z, Member S, Wu L, Fu Y. Real-time price-based demand response management for residential appliances via stochastic optimization and robust optimization 2012;3(4):1822–31.
[21] Lehrstuhl für Energiewirtschaft und Anwendungstechnik. e-MOBILie - Schaufenster Elektromobilität. <http://www.ewk.ei.tum.de/forschung/projekte/e-mobilie/>.
[22] Honold J, Kandler C, Wimmer P, Schropp B, Reichle R, Gröne M, Bünemann M, Klein J, Kufner M. Distributed integrated energy management systems in residential buildings. Appl Therm Eng 2017;114:1468–75. https://doi.org/10.1016/j.applthermaleng.2016.10.158.
[23] Olivares DE, Canizares CA, Kazerani M. A centralized energy management system for isolated microgrids. IEEE Trans Smart Grid 2014;5(4):1864–75. https://doi.org/10.1109/TSG.2013.2294187.
[24] Kok K, Widergren S. A society of devices: integrating intelligent distributed resources with transactive energy. IEEE Power Energy Mag 2016;14(3):34–45. https://doi.org/10.1109/MPE.2016.2524962.
[25] El-Baz W, Tzscheutschler P. Autonomous coordination of smart buildings in microgrids based on a double-sided auction. 2017 IEEE power & energy society general meeting, no. August Chicago: IEEE; 2017. p. 1–5. https://doi.org/10.1109/PESGM.2017.8273944.
[26] Bundesregierung. Gesetz zur Digitalisierung der Energiewende. Bundesgesetzblatt 2016;2016(43):2034–2064..
[27] Kriukov A, Vicol B, Gavrilas M. Applying a micro-market inside an electric vehicles parking facility. In: Proceedings of the Universities power engineering conference. doi:https://doi.org/10.1109/UPEC.2014.6934793.
[28] Kang J, Yu R, Huang X, Maharjan S, Zhang Y, Hossain E. Enabling localized peer-to-peer electricity trading among plug-in hybrid electric vehicles using consortium blockchains. IEEE Trans Ind Inform 2017;13(6):3154–64. https://doi.org/10.1109/TII.2017.2709784.
[29] Bahrami S, Amini MH. A decentralized trading algorithm for an electricity market with generation uncertainty. Appl Energy 2018;218(February):520–32. https://doi.org/10.1016/j.apenergy.2018.02.157. Available from: arXiv:1705.02577.
[30] Chen Y, Wei W, Liu F, Sauma EE, Mei S. Energy trading and market equilibrium in integrated heat-power distribution systems. IEEE Trans Smart Grid 2018;PP(c):1. https://doi.org/10.1109/TSG.2018.2849227.
[31] De Paola A, Angeli D, Strbac G. Price-based schemes for distributed coordination of flexible demand in the electricity market. IEEE Trans Smart Grid 2017;8(6):1386–93. https://doi.org/10.1109/CDC.2017.8263848.
[32] Long C, Wu J, Zhou Y, Jenkins N. Peer-to-peer energy sharing through a two-stage aggregated battery control in a community Microgrid. Appl Energy 2018;226(March):261–76. https://doi.org/10.1016/j.apenergy.2018.05.097.
[33] Khorasany M, Mishra Y, Ledwich G. Auction based energy trading in transactive energy market with active participation of prosumers and consumers. 2017 Australasian Universities Power Engineering Conference (Aupec). doi:https://doi.org/10.1109/AUPEC.2017.8282470.
[34] Kou W, Park SY. Game-theoretic approach for smartgrid energy trading with microgrids during restoration. IEEE power energy society general meeting 2018-Janua 2018. p. 1–5. https://doi.org/10.1109/PESGM.2017.8274437.
[35] Zhang C, Wu J, Zhou Y, Cheng M, Long C. Peer-to-peer energy trading in a microgrid. Appl Energy 2018;220(February):1–12. https://doi.org/10.1016/j.apenergy.2018.03.010.
[36] Tushar W, Yuen C, Mohsenian-Rad H, Saha T, Poor HV, Wood KL. Transforming energy networks via peer to peer energy trading: potential of game theoretic approaches. IEEE Signal Process Mag 2018;35(July):90–111. https://doi.org/10.1109/MSP.2018.2818327. Available from: arXiv:1804.00962.
[37] Millisterfer M. Transaktive Kontrolle in Projekten und Aktuellen Umsetzungen (Bachelor Arbeit). Technical University of Munich; 2018.
[38] Mengelkamp E, Gärttner J, Rock K, Kessler S, Orsini L, Weinhardt C. Designing microgrid energy markets: a case study: the Brooklyn microgrid. Appl Energy 2018;210:870–80. https://doi.org/10.1016/j.apenergy.2017.06.054.
[39] Morstyn T, Teytelboym A, McCulloch MD. Bilateral contract networks for peer-to-peer energy trading. IEEE Trans Smart Grid 2018;3053(c):1–10. https://doi.org/10.1109/TSG.2017.2786668.
[40] El-Baz W, Tzscheutschler P, Wagner U. Day-ahead probabilistic PV generation forecast for buildings energy management systems. Solar Energy 171. doi:https://doi.org/10.1016/j.solener.2018.06.100.
[41] El-Baz W, Eldakadosi M, Eren C. P3- prediction system. doi:https://doi.org/10.5281/ZENODO.1412785. <https://welbaz.github.io/p3/>.
[42] El-Baz W, Tzscheutschler P, Wagner U. Experimental study and modeling of ground-source heat pumps with combi-storage in buildings. Energies 11(5). doi:https://doi.org/10.3390/en11051174.
[43] Nymeyer IF. United States Patent, 723.
[44] Devine DG, Marion BW. The influence of consumer price information on retail pricing and consumer behavior: reply. Am J Agric Econ 1980;62(2):267. https://doi.org/10.2307/1239699.
[45] Cason TN, Friedman D. Price formation in double auction markets. J Econ Dyn Control 1996;20(8):1307–37. https://doi.org/10.1016/0165-1889(95)00901-9.
[46] Jadhav AM, Patne NR, Guerrero JM. A novel approach to neighborhood fair energy trading in a distribution network of multiple microgrid clusters. IEEE Trans. Ind Electron 0046(c). doi:https://doi.org/10.1109/TIE.2018.2815945.
[47] Goncalves Da Silva P, Ilic D, Karnouskos S. The impact of smart grid prosumer grouping on forecasting accuracy and its benefits for local electricity market trading. IEEE Trans Smart Grid 2014;5(1):402–10. https://doi.org/10.1109/TSG.2013.2278868.
[48] Faqiry MN, Member S, Das S. Double-sided energy auction in microgrid: equilibrium under price anticipation.
[49] Zhou Y, Wu J, Long C. Evaluation of peer-to-peer energy sharing mechanisms based on a multiagent simulation framework. Appl Energy 2018;222(February):993–1022. https://doi.org/10.1016/j.apenergy.2018.02.089.
[50] Shoham Y, Leyton-Brown K. Multiagent systems vol. 8953. Shoham and Leyton-Brown; 2008.
[51] Friedman DP, Rust J. The double auction market: institutions, theories, and evidence. Santa Fe Institute studies in the sciences of complexity proceedings, vol. 1993. Routledge; 1993. p. 103. https://doi.org/10.1016/j.joms.2013.02.009.
[52] Haas M, Zoican M-A. Discrete or continuous trading? HFT competition and liquidity on batch auction markets. Working Paper.
[53] Asare-Bediako B, Kling W, Ribeiro P. Multi-agent system architecture for smart home energy management and optimization. IEEE PES ISGT Europe 2013; 2013. p. 1–5. doi:https://doi.org/10.1109/ISGTEurope.2013.6695331.
[54] El-Baz W, Tzscheutschler P. Co-simulation of a smart home model based on a micro electricity market. In: Proceedings of the fifth German-Austrian IBPSA conference RWTH Aachen University; 2014. p. 30–7.
[55] Oberleitner S. Impact of country-specific requirements on the costs of charging

stations infrastructure (Bachelor Thesis); 2017.
[56] Lipp J, Sänger F. Potential of power shifting using a micro-CHP units and heat storages. Microgen3, Naples, Italy; 2013.
[57] El-Baz W, Seufzger M, Lutzenberger S, Tzscheutschler P, Wagner U. Impact of probabilistic small-scale photovoltaic generation forecast on energy management systems. Solar Energy 165. doi:https://doi.org/10.1016/j.solener.2018.02.069.
[58] Hilding Elmqvist. Modelica — a unified object-oriented language for physical systems modeling. Simul Pract Theory 1997;5(6):p32. https://doi.org/10.1016/S0928-4869(97)84257-7 <http://linkinghub.elsevier.com/retrieve/pii/S0928486997842577>.
[59] Hindmarsh AC, Serban R, Reynolds DR. User documentation for cvode v4.0.1 (sundials v4.0.1). Tech rep; 2018. <https://computation.llnl.gov/sites/default/files/public/cv_guide.pdf>.
[60] Najafi M, Nikoukhah R, Voluceau DD. Modeling and simulation of differential equations in Scicos. Model Assoc 2006(1):177–85.
[61] Lipp JP. Flexible Stromerzeugung mit Mikro-KWK-Anlagen; 2015.
[62] El-Baz W, Honold J, Hardi L, Tzscheutschler P. High-resolution dataset for building energy management systems applications. Data Brief 2018;54:1–5. https://doi.org/10.1016/j.dib.2017.12.058.
[63] ESI ITI. SimulationX 3.8 — Green City.
[64] EPISCOPE. IEE Project TABULA.
[65] Tjaden T, Bergner J, Weniger J, Quaschning V. Representative electrical load profiles of residential buildings in Germany with a temporal resolution of one second. Working paper. HTW Berlin -HTW Berlin - University of Applied Sciences Research; 2015. p. 1–7. doi:https://doi.org/10.13140/RG.2.1.5112.0080.
[66] Lipp J, Jungwirth J. Field test with stirling engine micro-CHP-units in residential buildings. MicroGEN II conference.
[67] BSW Solar. EEG 2017 - feste Einspeise- vergütungen im Überblick vergütungen im Überblick ∗ (April); 2018. p. 1–2.
[68] Kiesel L. Optimal occupancy based heating algorithm for multiple single family home types (Bachelor Thesis); 2015.